BIOMASS AND BIOENERGY XXX (2010) 1–11

Available at www.sciencedirect.com

http://www.elsevier.com/locate/biombioe

Changes in lignocellulosic supramolecular and ultrastructure during dilute acid pretreatment of *Populus* and switchgrass

*Marcus Foston, Art J. Ragauskas**

BioEnergy Science Center, School of Chemistry and Biochemistry, Institute of Paper Science and Technology, Georgia Institute of Technology, 500 10th St., Atlanta, GA 30332, USA

ARTICLE INFO

Article history:
Received 23 March 2009
Received in revised form
17 July 2010
Accepted 23 July 2010
Available online xxx

Keywords:
Dilute acid pretreatment
Cellulose
Supramolecular structure
Populus
Switchgrass

ABSTRACT

Dilute acid pretreatment (DAP) is commonly employed prior to enzymatic deconstruction of cellulose to increase overall sugar and subsequent ethanol yields from downstream bioconversion processes. Typically optimization of pretreatment is evaluated by determining hemicellulose removal, subsequent reactivity towards enzymatic deconstruction, and recoverable polysaccharide yields. In this study, the affect of DAP on the supramolecular and ultrastructure of lignocellulosic biomass was evaluated. A series of dilute acidic pretreatments, employing ~0.10–0.20 mol/m^3 H_2SO_4 at ~160–180 °C, for varying residence times were conducted on both *Populus* and switchgrass samples. The untreated and pretreated biomass samples were characterized by carbohydrate and lignin analysis, gel permeation chromatography (GPC) and ^{13}C cross polarization magic angle spinning (CPMAS) NMR spectroscopy. GPC analysis shows a reduction in the molecular weight of cellulose and change in its polydispersity index (PDI) with increasing residence time, indicating that pretreatment is actually degrading the cellulose chains. ^{13}C CPMAS and non-linear line-fitting of the C_4 region in the carbon spectrum of the isolated cellulose not only showed that the crystallinity index increases with residence time, but that the lateral fibril dimension (LFD) and lateral fibril aggregate dimension (LFAD) increase as well.

1. Introduction

Lignocellulosic biomass may be used as a potential source of renewable energy via biochemical conversion of cellulose to second generation biofuels like cellulosic ethanol. Many lignocellulosic raw materials, such as *Populus* and switchgrass, have been evaluated for their potential bioconversion as biomass energy crops. Cellulose can effectively be deconstructed by enzymatic hydrolysis into its constituent monomer and fermented to ethanol. The structure of lignocellulosics occurs as a complex microstructure system composed of lignin and hemicellulose matrix encapsulating and supporting cellulose fibrils packed into bundles. The cellulose fibril themselves are a mixture of ordered and unordered regions [1,2]. Adding to the structural complexity, X-ray and neutron diffraction studies have provided information suggesting multiple crystalline allomorphs such as cellulose I_α and I_β exist in native cellulose [3,4].

The economics of biofuel production is very dependent on the overall sugar yields and energy cost associated with biomass deconstruction. The very properties that make cellulose so useful in nature as a structural biopolymer in the cell walls of plants makes it difficult to deconstruct. The mechanisms of efficiently overcoming recalcitrance are therefore important to understand. Typically, prior to enzymatic hydrolysis and fermentation, biomass is subjected to

* *Corresponding author*. Tel.: +1 404 894 9701; fax: +1 404 894 4778.
E-mail address: Art.Ragauskas@chemistry.gatech.edu (A.J. Ragauskas).
0961-9534/$ – see front matter © 2010 Elsevier Ltd. All rights reserved.
doi:10.1016/j.biombioe.2010.07.023

pretreatment via physical and chemical means. The goal of this pretreatment is to homogenize biomass, open the lignin–hemicellulose matrix and disrupt the ultrastructure of the cellulose [5–10]. Ultimately, increasing enzymatic cellulose accessibility and reactivity is extremely critical.

DAP has been extensively studied as a pre-hydrolysis method and it has been reported that it removes hemicellulose, disrupts the lignin structure, and enhances deconstruction of cellulose [6–9]. DAP utilizes a combination of controlled pH, heat, and pressure to minimize lignin- and carbohydrate-degradation product formation which can cause an inhibitory effect on enzymatic activity [11], maximizing swelling and solublization of hemicellulose. The general principles of DAP are illustrated in Fig. 1 which predicts how acidic pretreatment conditions not only could possibly impact hemicellulose structures but also the other biomass components. Such conditions will cause degradation, solublization and/or transformation, whether advantageous or not within various components of the biomass.

Many traditional pretreatment studies suggest that optimization of hemicellulose removal and lignin disruption can be achieved by adjusting pretreatment conditions [7–9]. Moreover, ^{13}C CPMAS NMR studies reported that changes were observed in cellulase activity with ultrastructural features of cellulose [13]. These results indicate that it may be possible to optimize the changes in ultrastructure to further increase downstream yields.

NMR has been used to analyze the ultrastructure of cellulose for almost three decades. Early work by Attala and Vanderhart recognized ^{13}C CPMAS NMR as a potential technique to investigate native cellulose [14,15]. They used high resolution solid-state NMR to identify several resonances that were attributed to the various carbons on cellulose [1]. They also noticed the position and appearance of those resonances changed with the source of the cellulose. Utilizing a combination of information from crystallographic studies, Raman and NMR spectroscopy it was determined that these changes correspond to the natural enrichment of particular crystalline allomorphs within the native cellulose [1,16,17].

In later studies, the molecular order in cellulose was investigated by determining the appearance of crystalline and non-crystalline sub-spectra based upon variations in chemical shift and ^{13}C relaxation [18]. The NMR spectra of lignocellulosic samples, much like other biological material, are fairly complex containing multiple broad and overlapping peaks. This problem was addressed by using a least-squared model and spectral fitting method which was established to quantitatively estimate the relative fraction of ultrastructural components [19]. Several researchers, including Iverson, Wickholm and Larrson, have since used and refined this model and method. Over the years it has evolved to include the non-linear line-fitting of seven resonances of adjustable shape, width, chemical shift, and relative intensity. Each resonance represents either a crystalline domain of cellulose I_α, I_β or *para*-crystalline cellulose or amorphous domain of accessible or inaccessible fibril surfaces [20–24].

Information extracted from ^{13}C CPMAS NMR can not only provide the relative amounts of cellulose allomorphs present, but can also be used to determine the average lateral dimensions of fibril and fibril aggregates [20,24–29]. The use of ^{13}C CPMAS NMR is not simply for cataloging ultrastructural differences in native or modified cellulose. It has also been applied in comparative studies, such as investigating whether kraft or sulphite pulping changes the supramolecular structure of wood [20,30–34].

Similarly in this study, we present the use of ^{13}C CPMAS NMR in combination with GPC on isolated cellulose and compositional analysis as tools to track the changes in lignocellulosic supramolecular and ultrastructure during dilute acid pretreatment of *Populus* and switchgrass. By understanding the nature and kinetics of the various reactions/transformation in Fig. 1 and how those processes respond to various pretreatment conditions, an optimized substrate for enzymatic deconstruction can be effectively generated. Biomass samples were treated as a 5 wt.% slurry in dilute acid and heated in a pressure reactor for varying residence times and then characterized by GPC and ^{13}C CPMAS NMR in an attempt to understand the changes in biomass structure occurring during pretreatment. Ultimately, characterizing and comprehending these substrate changes and the subsequent relationship between lowered recalcitrance will enable the development of a more effective pretreatment system.

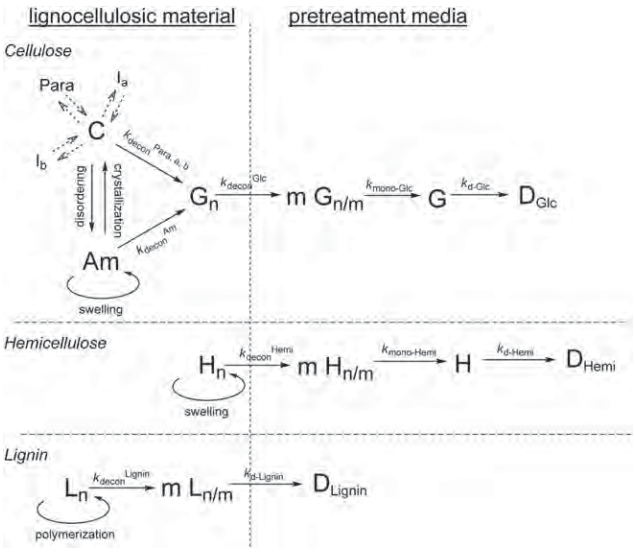

Fig. 1 – A model that represents the hydrolyzation reactions and probable changes observed in the supramolecular structure of lignocellulosics during DAP (adapted from a figure in Ref. [12]).

2. Materials and methods

2.1. Substrates

Baseline *Populus* (*Populus trichocarpa x deltoides*) and lowland cultivar Alamo switchgrass (*Panicum virgatum*) samples were harvested between 2007–2008 from area 0800 at Oak Ridge National Laboratory, TN. The samples were then shipped to the National Renewable Energy Laboratory (NREL) in Golden, CO for room temperature air drying, de-barking (for poplar)

Please cite this article in press as: Foston M, Ragauskas AJ, Changes in lignocellulosic supramolecular and ultrastructure during dilute acid pretreatment of *Populus* and switchgrass, Biomass and Bioenergy (2010), doi:10.1016/j.biombioe.2010.07.023

and size-reduction. The samples were stored in a freezer to maintain the moisture content and shipped to Georgia Tech upon request. The biomass was sized-reduced in a Wiley mill using a 20–80 mesh screen. Extractives were subsequently removed by placing 5 g of biomass into an extraction thimble in a Soxhlet extraction apparatus. The extraction flask was filled with 1:2 ethanol/benzene mixture (~150 mL) and then refluxed at a boiling rate which cycled the biomass for at least 24 extractions over a 4 h period.

2.2. Dilute acid pretreatment (DAP)

Lignocellulosic samples were first prepared by pre-soaking, which was done at 25 °C while continuously stirring in a ~0.10 mol/m^3 dilute sulfuric acid solution at 5% dry extractive-free and size-reduced lignocellulosic solids (w of solids/w of suspension) for 4 h. The pre-soaked slurry was filtered to remove the solid material and washed with an excess of de-ionized (DI) filtered water. 2.00 g of the pre-soaked material (by dry mass) was transferred to a 4560 mini-Parr 300 mL pressure reactor with ~0.10 or 0.20 mol/m^3 H_2SO_4 solutions at 5% dry solids and was then sealed under ambient atmospheric conditions. The impeller speed was set to about 1.67 Hz, and the vessel was heated to 160, 175 or 180 °C over ~25–30 min (at ~6 °C min^{-1}). The reactor was held at the pretreatment temperature ±2 °C (~650–690 kPa) for the specified residence time ±30 s (2.5, 5, 10, 20 and 60 min). The reactor was then quenched in an ice bath (~5 min) and then vented. The pretreated slurry was filtered to remove the solid material and washed with an excess of DI filtered water. The pretreated lignocellulosic samples were dried in the fumehood overnight at room temperature. Paramagnetic impurities were removed by washing the solids with a 2 wt.% aqueous solution of ethylenediaminetetraacetic acid (EDTA) and DI filtered water. All yields for biomass recovered after pretreatment ranged between 55 and 75% by mass of dry extractive-free and size-reduced lignocellulosic solids.

2.2.1. Sample preparation for NMR

Isolated cellulose was generated by first preparing holocellulose from Wiley milled *Populus* and switchgrass. This milled biomass this treated with $NaClO_2$ (1.30 g/1.00 g lignocellulosic dry solids) in acetic acid (375 mL of 0.14 mol/m^3) at 70 °C for 2 h. The samples were then collected by filtration and rinsed with an excess of DI filtered water. This procedure was repeated to ensure complete removal of the lignin component. Isolated cellulose was prepared from the holocellulose sample (1.00 g) by acid hydrolysis for 4 h in HCl (100.0 mL of 2.5 mol/m^3) at 100 °C. The isolated cellulose samples were then collected by filtration and rinsed with an excess of DI filtered water, and dried in the fumehood at room temperature.

2.2.2. Sample preparation for gel permeation chromatography (GPC)

Isolated α-cellulose was generated by first isolating holocellulose from milled biomass pulp using the above method. Isolated cellulose was prepared from the holocellulose sample (1.00 g) by extraction with a 17.5 wt.% NaOH solution (50 mL) at 25 °C for 30 min. 50 mL of DI filtered water was then added to the NaOH solution. The extraction was continued with the 8.75 wt.% NaOH solution (100.00 mL) at 25 °C for an additional 30 min. The isolated α-cellulose samples were then collected by filtration and rinsed with 50 mL of 1 wt.% acetic acid, an excess of DI filtered water, and dried in the fume hood at room temperature.

2.2.3. ^{13}C CPMAS NMR analysis of cellulose

The NMR samples were prepared with ground isolated cellulose added into 4-mm cylindrical ceramic MAS rotors. Solid-state NMR measurements were carried out on a Bruker DSX-400 spectrometer operating at frequencies of 100.55 MHz for ^{13}C in a Bruker double-resonance MAS probehead at spinning speeds of 10 kHz. CPMAS experiments utilized a 5 μs (90°) proton pulse, 1.5 ms contact pulse, 4 s recycle delay and 4–8 K scans. All spectra were recorded on pre-wet samples (60–80% water content), and both a 2-peak (% crystallinity) and 7-peak line-fitting analysis of spectra was performed using NUTS NMR Data Processing software (Acorn NMR, Inc).

2.2.4. GPC analysis of cellulose

The number-average molecular weight (M_n) and weight-average molecular weight (M_w) were determined by GPC after tricarbanilation of cellulose. Lignin-free α-cellulose (15 mg) from each sample was placed in separate test tubes equipped with micro stir bars and dried overnight under vacuum at 40 °C. The test tubes were then capped with rubber septa. Anhydrous pyridine (4.00 mL) and phenyl isocyanate (0.50 mL) were added sequentially via syringe. The test tubes were placed in an oil bath at 70 °C and allowed to stir for 48 h. Methanol (1.00 mL) was then added to quench any remaining phenyl isocyanate. The contents of each test tube were then added drop wise to a 7:3 methanol/water mixture (100 mL) to promote precipitation of the derivatized cellulose. The solids were collected by filtration and then washed with methanol/water (1 × 50 mL) followed by water (2 × 50 mL). The derivatized cellulose was then dried overnight under vacuum at 40 °C [36]. Prior to GPC analysis the derivatized cellulose was dissolved in THF (1 mg/mL), filtered through a 0.45 μm filter and placed in a 2 mL auto-sampler vial.

The molecular weight distributions of the cellulose tricarbanilate samples were then analyzed on an Agilent GPC SECurity 1200 system equipped with four Waters Styragel columns (HR1, HR2, HR4, HR5), Agilent refractive index (RI) detector and Agilent UV detector (270 nm) using THF as the mobile phase (1.0 mL/min) with injection volumes of 20 μL. A calibration curve was constructed based on eight narrow polystyrene standards ranging in molecular weight from 1.5 × 10^3 to 3.6 × 10^6 g/mol. Data collection and processing were performed using Polymer Standards Service WinGPC Unity software (Build 6807). Molecular weights (M_n and M_w) were calculated by the software relative to the universal polystyrene calibration curve. Number-average degree of polymerization (DP_n) and weight-average degree of polymerization (DP_w) were obtained by dividing M_n and M_w by 519 g/mol, the molecular weight of the tricarbanilated cellulose repeat unit. Polydispersity index (PDI) was calculated by dividing M_w by M_n.

Please cite this article in press as: Foston M, Ragauskas AJ, Changes in lignocellulosic supramolecular and ultrastructure during dilute acid pretreatment of *Populus* and switchgrass, Biomass and Bioenergy (2010), doi:10.1016/j.biombioe.2010.07.023

2.2.5. *Carbohydrates and Klason lignin analysis*

Samples for carbohydrate constituents and acid-insoluble lignin (Klason lignin) analysis was prepared using a two-stage acid hydrolysis protocol based on TAPPI methods T-222 om-88 with a slight modification [35]. The first stage utilizes a severe pH and a low reaction temperature (72 vol.% H_2SO_4 at 30 °C for 1 h). The second stage is performed at much lower acid concentration and higher temperature (3 vol.% H_2SO_4 at 121 °C for 1 h) in an autoclave. The resulting solution was cooled to room temperature and filtered using G8 glass fiber filter (Fisher Scientific, USA). The remaining residue which is considered as Klason lignin was oven-dried at 105 °C and weighed to obtain the Klason lignin content. The filtered solution was analyzed for carbohydrate constituents of the hydrolyzed samples determined by high-performance anion-exchange chromatography with pulsed amperometric detection (HPAEC-PAD) using Dionex ICS-3000 (Dionex Corp., USA).

2.2.6. *Error analysis*

An experimental error analysis procedure was conducted by performing three individual pretreatments for the 5 min data point. Based on the results of the NMR line-fitting, carbohydrate/lignin and GPC analysis typical errors associated with the pretreatment of lignocellulosics, holocellulose pulping, and hemicellulose hydrolysis were calculated equaling one standard deviation of the three 5 min data point trials. The typical error associated with NMR measurements with respect to the % relative intensity of the total crystalline allomorphs, *para*-crystalline and amorphous domains was 4.5, 0.8 and 2.5% respectively. NMR acquisitions and 2-peak line-fit data processing indicate % crystallinity can be determined within ±2%. The typical error associated with carbohydrate and lignin analysis with respect to the % relative amount of xylose, mannose, arabinose, galactose, glucose and lignin was ±5.8, 1.2, 0.2, 0.1, 7.1 and 4.8% respectively. The error associated with GPC analysis with respect to the M_n and M_w was ±11 and 30 g/mol respectively.

3. Results and discussion

3.1. *Carbohydrates and lignin analysis*

DAP is viewed as a tool to increase the effectiveness of downstream processing (such as enzymatic deconstruction) of biomass energy crops. Therefore, *Populus* and switchgrass samples were pretreated varying experimental parameters such as time, temperature and the acid concentration of the pretreatment to not only achieve controlled variations but to also understand the origin and extent of those variations within the ultrastructure of lignocellulosics.

As shown in Fig. 2, the *Populus* and switchgrass samples when exposed to DAP conditions change in the material brightness and color. As pretreatment residence times are increased, the material becomes increasingly dark-brown in appearance. The pretreatment conditions were anticipated to impart equally dramatic changes in the various chemical components in lignocellulosics whose magnitude may be related to pretreatment residence time. Previous studies have linked this type of color change to the chemical degradation of carbohydrates, lignin, and wood extractives, wood extractives [37].

In an effort to quantitatively analyze the changes in the composition of the structural carbohydrates and lignin, which make up a major portion of the biomass samples, monosaccharide and Klason lignin analysis were performed. Fig. 3a and b summarize the changes in carbohydrate and lignin distribution before and after pretreatment. According to Fig. 3, the majority of the hemicellulose, typically characterized by the xylose, mannose, arabinose, and galactose contents, for both the *Populus* and switchgrass samples, is removed within 2.5–5 min of DAP. Although switchgrass displayed a slightly higher hemicellulose content before pretreatment, the observed hemicellulose hydrolyzation rate was very similar to that of *Populus*.

At 5–10 min of DAP for both samples the glucose content reaches a maximum indicating that subsequent to this time frame the hydrolyzation of cellulose and subsequent solubilization of glucose becomes the dominate process. The lignin content also significantly increases, indicating the pretreatment is fairly ineffective at removal of the majority of lignin. The large increases seem to suggest appreciable cellulose is hydrolyzed, however the results of acid insoluble (Klason) lignin contents could be misleading for the pretreated samples. It was reported only half of the Klason lignin extracted by a dioxane–water solvent system from a hot water pretreated biomass was actual lignin, suggesting the remaining 'pseudo-lignin' material might have been produced as result of repolymerization of polysaccharide degradation products forming lignin-like polyphenolic structures [38].

A final comment on the pretreatment procedure is related to the pre-soaking of biomass samples as part of DAP. The lignocellulosic samples were pre-soaked before pretreatment in ~0.10 mol/m^3 H_2SO_4 solution at room temperature for 4 h. Previous research pertaining to optimization of conditions for DAP has shown this initial impregnation helps eliminate appreciable transport affects [39].

3.2. *GPC of* Populus *and switchgrass pre and post pretreatment*

GPC is frequently employed to determine the molecular weight distribution (MWD) of cellulose in lignocellulosics [36,40,41]. Various studies have shown GPC to be a valuable tool in monitoring degradation of not only cellulose but also hemicellulose and lignin[42–44]. Table 1 shows the weight-number molecular weight (M_w) and polydispersity index (PDI) resulting from the integration of the GPC chromatographs of isolated cellulose modified with phenyl isocyanate prepared from *Populus* and switchgrass under DAP conditions of increasing residence times. The chromatographs show a bimodal MWD with a major peak centered at a molecular weight of 100,000 g/mol for untreated *Populus* and switchgrass respectively. There is a general retention time shift of the major peak to longer retention times or lower molecular weight. This would indicate that DAP is reducing the M_w and degrading polysaccharides by chain scission within the fibril structure. As the residence time is increased the data in Table 1 shows this degradation becomes fairly appreciable.

Please cite this article in press as: Foston M, Ragauskas AJ, Changes in lignocellulosic supramolecular and ultrastructure during dilute acid pretreatment of *Populus* and switchgrass, Biomass and Bioenergy (2010), doi:10.1016/j.biombioe.2010.07.023

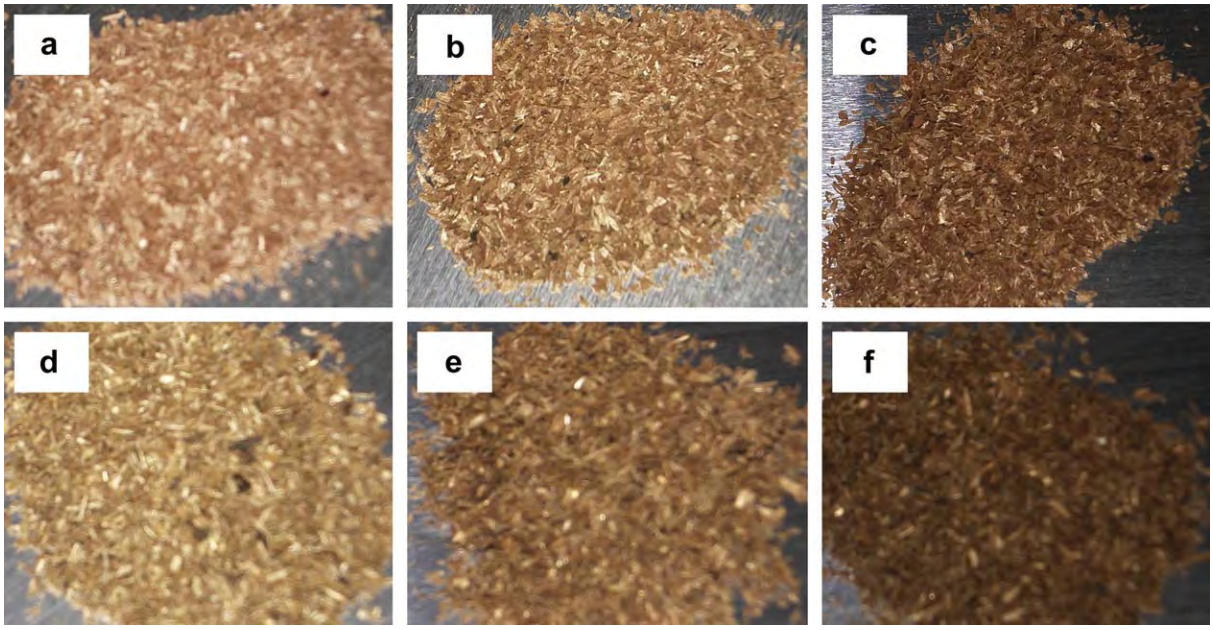

Fig. 2 – Lignocellulosic samples after DAP in a ~0.10 mol/m^3 H_2SO_4 solution at 160 °C for *Populus* at (a) 2.5, (b) 5, (c) 10 min and switchgrass at (d) 2.5, (e) 5, (f) 10 min.

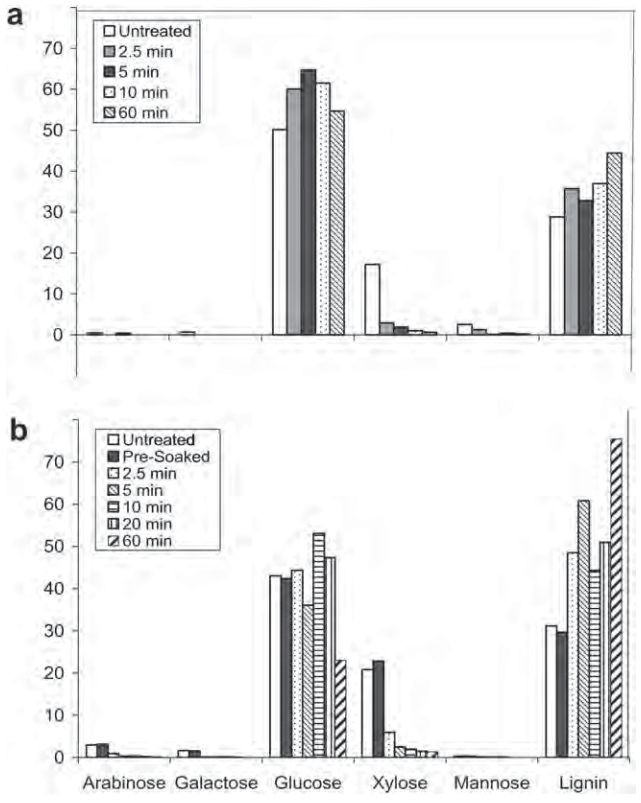

Fig. 3 – Carbohydrate and Klason lignin content of (a) *Populus* and (b) switchgrass after DAP in ~0.10 mol/m^3 H_2SO_4 solution at 160 °C.

According to the model in Fig. 1, the degradation pathway of cellulose can be viewed as acid catalyzed, thermally accelerated polysaccharide hydrolysis from within either a crystalline or amorphous region. In a study on the hydrolysis of the amorphous cellulose in cotton-based paper, it was determined the overall degradation process can be considered as having two major stages. The initial stage was described as rapid hydrolytic attack on the more solvent accessible amorphous chain segments, while the latter "leveled-off" stage displays a much slower kinetic of hydrolytic attack on and/or at crystal surfaces [42,45]. Kinetic Monte Carlo simulations of cellulose degradation corroborated the observations of strength loss determined by uniaxial tensile testing due to reduction in molecular weight analyzed via GPC and electrospray ionization-mass spectrometry. The simulations were based on predictions developed for a semi-crystalline material, in which the changes in material properties are not a function of the total number of cellulose chains but rather

Table 1 – GPC results from the integration of the chromatographs of isolated cellulose modified with phenyl isocyanate prepared from poplar and switchgrass after DAP in ~0.10 mol/m^3 H_2SO_4 solution at 160 °C.

	Populus			Switchgrass		
Pretreatment Time (min)	M_w (g/mol)	PDI	DP_w	M_w (g/mol)	PDI	DP_w
0	1065000	9.2	2076	970000	29.6	1891
2.5	356000	11.0	694	1008000	25.4	1965
5	352000	8.6	686	688000	15.9	1342
10	201000	5.8	392	259000	9.5	506
20	–	–	–	293000	10.3	572
60	79000	4.5	154	150000	7.0	293

Please cite this article in press as: Foston M, Ragauskas AJ, Changes in lignocellulosic supramolecular and ultrastructure during dilute acid pretreatment of *Populus* and switchgrass, Biomass and Bioenergy (2010), doi:10.1016/j.biombioe.2010.07.023

the number of intact amorphous chains between crystalline domains [42]. In conjunction with common accessibility and reactivity arguments [1,2,46], this work confirmed spatially localized hydrolysis in the amorphous regions occurs during acidic hydrolysis of cellulose.

The curve in Fig. 4 shows the number of chain breaks per original cellulose chain during pretreatment with the solid lines representing a non-linear regression fit to an exponential model. The number of chain breaks per original chain was calculated by taking the ratio of the weight-average molecular weight of the untreated sample to that of the pretreated samples ($=[M_n^0/M_n] - 1$). The kinetics of cellulose degradation can clearly be seen in Fig. 4 as the plot seemingly indicate a leveling-off of acid hydrolysis will occur at long pretreatment times.

3.3. CPMAS ^{13}C NMR spectroscopy

A series of ^{13}C CPMAS NMR spectroscopy experiments were conducted to determine the relative intensity of the ultrastructural components within cellulose fibrils and how those relative intensities change with residence time for pretreated *Populus* and switchgrass samples (ultrastructural components of cellulose: cellulose I_α and I_β, *para*-crystalline cellulose and cellulose at accessible and inaccessible surface). Fig. 5 provides a representative spectrum of isolated cellulose prepared from *Populus* after holocellulose pulping and hemicellulose hydrolysis.

Each of the six carbon atoms in the monomeric unit of the cellulose backbone are denoted C_1 through C_6 and labeled accordingly on the corresponding carbon signal in the spectrum. The C_4 region, which extends over a chemical shift range of $\delta \sim 80$–92 ppm, is commonly used to probe cellulose amorphous domains which appear as fairly broad signals from $\delta \sim 80$–85 ppm and crystalline domains that produce sharper, slightly upfield resonances [1,17]. Fig. 6 shows the non-linear least-squared line-fitting of the C_4 region for a ^{13}C CPMAS spectrum of isolated cellulose prepared from *Populus* after 2.5 min of DAP in ~0.10 mol/m^3 H_2SO_4 solution at 160 °C.

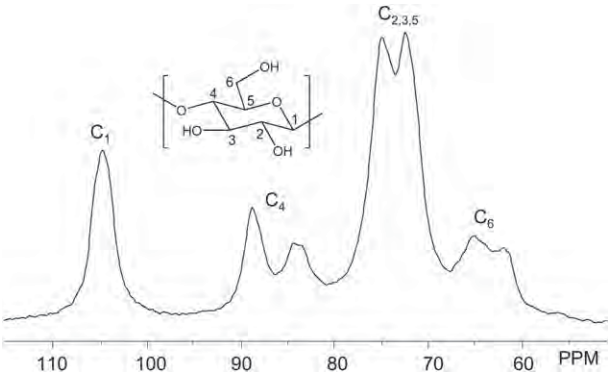

Fig. 5 – A representative ^{13}C CPMAS spectrum of isolated cellulose from untreated *Populus*.

Lorentzian line-shapes were applied to the carbon signals attributed to domains of cellulose $I_{\alpha+\beta}$, I_α, I_β and *para*-crystalline cellulose, while Gaussian lines were used to describe the signals from inaccessible and accessible fibril surfaces comprising the amorphous domains. The results of this fitting procedure on pretreated *Populus* are compiled in Table 2. The chemical shift assignments determined for the untreated samples of *Populus* and switchgrass were used in analyzing the other ^{13}C spectra of the pretreated samples.

3.3.1. Crystalline cellulose

Fig. 7 shows the relative intensity of the combined crystalline allomorphs ($=\%I_{\alpha+\beta} + \%I_\alpha + \%I_\beta$) and *para*-crystalline form. The data from *Populus* and switchgrass samples are plotted against their pretreatment combined severity factor (CSF), which is a value calculated to combine the parameters of time, temperature, and pretreatment bath pH into a single reaction ordinate, in order to compare pretreatments of varying severity despite the particular combination of pretreatment conditions [9]. Both this data and the data in Fig. 9, is described in terms of CSF because three *Populus*

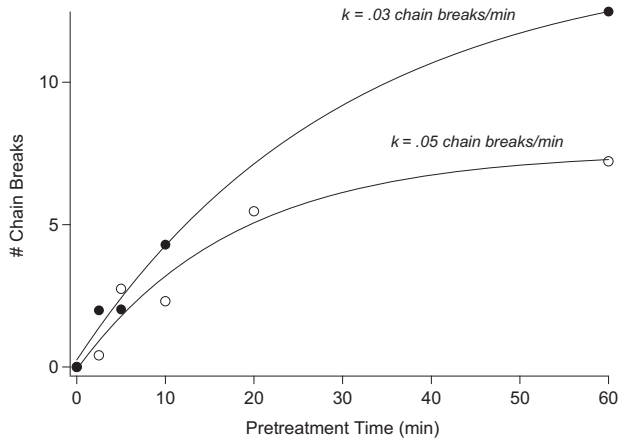

Fig. 4 – Number of chain breaks per original cellulose chain for (●) *Populus* and (○) switchgrass as a result of DAP in ~0.10 mol/m^3 H_2SO_4 solution at 160 °C. The lines are fits to an exponential model.

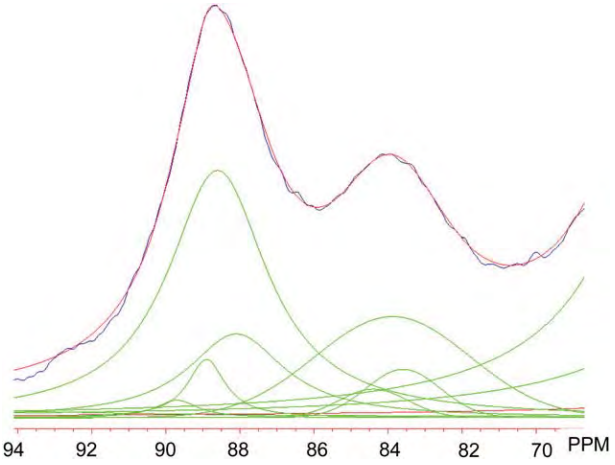

Fig. 6 – The non-linear, least-squared, spectral fitting of the C_4 region of ^{13}C CPMAS spectrum of isolated cellulose from *Populus* after 2.5 min of DAP in ~0.10 mol/m^3 H_2SO_4 solution at 160 °C.

Please cite this article in press as: Foston M, Ragauskas AJ, Changes in lignocellulosic supramolecular and ultrastructure during dilute acid pretreatment of *Populus* and switchgrass, Biomass and Bioenergy (2010), doi:10.1016/j.biombioe.2010.07.023

Table 2 – Non-linear least-squared spectral fitting results of the C_4 region for ^{13}C CPMAS spectra of isolated cellulose from *Populus* after 5 min of DAP in ~0.10 mol/m^3 H_2SO_4 solution at 160 °C. The values in the parenthesis represent the standard deviation of three separate samples pretreated for 5 min.

Assignment	Chemical shift (ppm)	Relative intensity (%)	Full-width at half-maximum (Hz)
I_α	89.7	1.9 (2.7)	34 (11)
$I_{(\alpha+\beta)}$	88.9	9.4 (1.0)	96 (24)
Para-crystalline	88.6	42.0 (0.8)	246 (57)
I_β	88.1	17.1 (1.3)	214 (30)
Accessible fibril	84.4	4.1 (0.9)	196 (67)
Inaccessible fibril	83.9	17.9 (0.7)	441 (99)
Accessible fibril	83.6	7.5 (0.6)	186 (22)

samples were pretreated at higher temperatures (>160 °C) and/or lower pH (>0.10 mol/m^3 H_2SO_4), but having similar CSF values in an attempt to more independently evaluate the affect of temperature and pH during DAP on the ultrastructure of cellulose.

Para-crystalline cellulose is loosely described as chain segments having more-order and less mobility than amorphous chains segments but less-ordered and more mobile

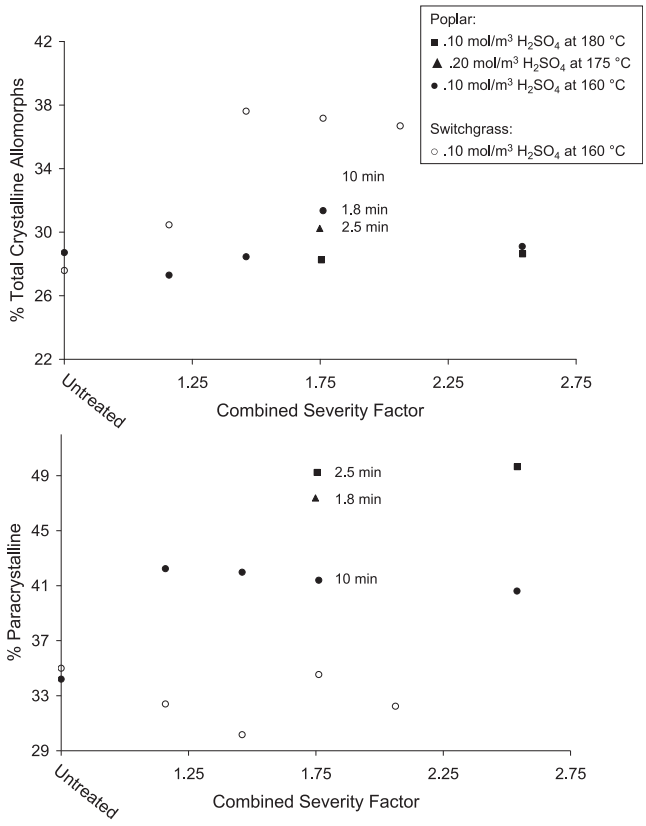

Fig. 7 – The crystalline and *para*-crystalline content as determined by spectral fitting of the C_4 region of ^{13}C CPMAS spectra of isolated cellulose from *Populus* and switchgrass after DAP in a H_2SO_4 solution under varying acidic conditions as defined by the combined severity factor.

than chains within crystals [23,42]. The existence of such regions was developed based on ^{13}C CP NMR pulse sequences that can differentiate between sample components with different T_1 or T_2 relaxations [43]. As seen in Fig. 7, the relative proportion of *para*-crystalline cellulose increases over the initial 2.5 min of pretreatment for the *Populus* samples, while remaining fairly constant for the switchgrass samples. The *Populus* data points having CSF values of ~1.75 and 2.54 suggests that temperature may be the critical rate determining parameter, demonstrating a *para*-crystalline content that seems to increase with temperature increase.

In addition, the % combined crystalline allomorph seen in Fig. 7 seems to remain fairly constant during DAP for *Populus*. However the plot does indicate switchgrass has a slight increase in the proportion of total crystalline allomorphs, at least within the first 20 min of DAP. Based upon the conclusions made via GPC and kinetic studies of the hydrolysis of cellulose, the majority of the increase in crystallinity and *para*-crystalline percentage is primarily due to localized hydrolyzation and removal of cellulose in the amorphous regions. However, as described in the model in Fig. 1, the relative proportion of both the crystalline and *para*-crystalline forms can also be affected by ultrastructural transformation mechanisms and/or hydrolyzation at crystalline surfaces. The *Populus* data point at CSF values of ~1.75 and 2.54 indicates what seems to be a decrease in % combined crystalline allomorph with temperature increase.

Both *Populus* and switchgrass showed that while the relative intensity for the other crystalline allomorphs increases with residence time, the relative intensity of the cellulose I_α form decreases. This suggests the cellulose I_α form is susceptible to either selective degradation by acidic hydrolyzation and/or transformation to other crystal allomorphs during pretreatment. On the basis of ^{13}C CPMAS NMR, it was noted native Valonia cellulose was composed predominately of cellulose I_α, transformed into cellulose I_β crystals upon annealing above 260 °C with saturated steam (hydrothermal conditions) [44]. This transformation is attributed to the triclinic one-chain crystal structure of cellulose I_α, which is referred to as being "metastable", having less density and thermodynamic stability than the monoclinic two-chain cellulose I_β form [44–47]. Because it is unlikely that significant hydrolysis of the crystalline regions occurs during DAP [42,45] under the previously described time/temperature profile, the changes seen in the relative proportion of the crystalline allomorphs and *para*-crystalline cellulose are at least partly due to either this crystal-to-crystal type of transformation or conversion to the less-ordered *para*-crystalline form.

To further clarify the origins of the observed changes in the relative proportion of the ultrastructural components, the ratio of actual changes in relative intensities to the expected changes based upon changes in amorphous content ($\Delta_{real}/\Delta_{theo}$), was calculated and plotted against pretreatment time in Fig. 8. Upon hydrolysis of amorphous cellulose, assuming that little or no crystalline material is removed, and minimal disordering of crystalline regions occur, the relative intensity of the crystalline allomorphs and *para*-crystalline cellulose should increase by a predictable percent via a simple mass balance. If the absolute value of $\Delta_{real}/\Delta_{theo} > 1$, the observed changes in relative intensity

Please cite this article in press as: Foston M, Ragauskas AJ, Changes in lignocellulosic supramolecular and ultrastructure during dilute acid pretreatment of *Populus* and switchgrass, Biomass and Bioenergy (2010), doi:10.1016/j.biombioe.2010.07.023

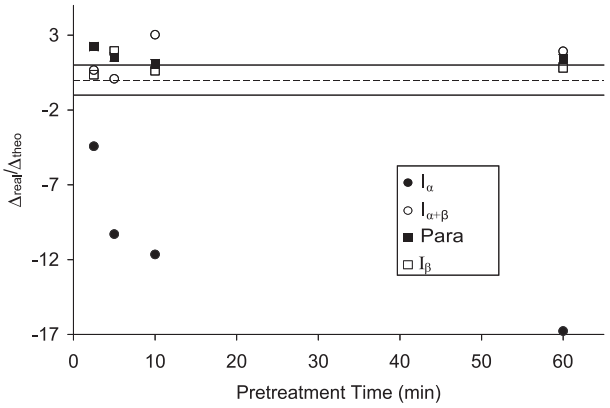

Fig. 8 – The ratio of actual changes in relative intensities to the expected changes in relative intensities based upon changes in amorphous content of various ultrastructural components in poplar during DAP. Solid horizontal line mark $\Delta_{real}/\Delta_{theo}$ values of 1 and −1, and the dotted horizontal line marks $\Delta_{real}/\Delta_{theo}$ value of 0.

is greater than it should be if the only process occurring is removal of amorphous chain segments by a factor of $\Delta_{real}/\Delta_{theo}$. If the absolute value of $\Delta_{real}/\Delta_{theo} < 1$, the observed changes in relative intensity is smaller than the expected changes by a factor of $\Delta_{real}/\Delta_{theo}^{-1}$. If the magnitude of $\Delta_{real}/\Delta_{theo}$ is negative the observed changes happened in the opposite direction of the expected changes. Each data point represents the changes occurring between that pretreatment time and the untreated data point.

The plot in Fig. 8 shows that within the first ~2.5 min of pretreatment for *Populus* the increase in *para*-crystalline content is almost triple that of the expected value, whereas the other crystalline allomorphs either show increases of half as much as expected or in the case of cellulose I_α actually demonstrate a decrease instead of an increase. As time progresses the plot indicates a continued reduction of cellulose I_α well-below expected values and *para*-crystalline cellulose to expected values. Data points at 5 min indicate the existence of an unproportionally high fraction of cellulose I_β, while data points at 60 min confirm all crystalline and *para*-crystalline cellulose contents are greater than expected. Based upon those observations in the initial 2.5 min of pretreatment cellulose I_α is primarily converted to *para*-crystalline cellulose. However, after the first 2.5 min, the majority of the cellulose I_α conversion is dominated by the formation of cellulose I_β, while simultaneously a small fraction of *para*-crystalline cellulose slowly begins to transform into crystalline cellulose, which continues for the duration of the pretreatment. This would suggest *para*-crystalline cellulose may be a metastable and persistent intermediate in crystalline allomorph transformation.

The final data points in Fig. 8 suggest that there is some mechanism other than crystalline transformation increasing the combined crystalline allomorph and *para*-crystalline contents. This is supported by work which show under hydrothermal conditions cellulose will undergo the opposing processes of crystallization and disordering, as depicted in Fig. 1. Under milder conditions, such as temperatures from 130 to 160 °C, it was shown that this equilibrium is shifted toward crystallization, while disordering primarily occurs at much higher temperatures [47,48]. Also, wood polymers have displayed softening in the dry state at temperature ranging from 180 to 250 °C [48]. Whereas, under wet conditions as low as 90 °C, spruce wood displays softening [49–51]. This is primarily associated with the loosening of the lignin–hemicellulose matrix, which would be a necessary precursor to any appreciable crystallization because of significant fibril enlargement [48].

3.3.2. *Amorphous cellulose*

The ultrastructural components in the amorphous regions of cellulose are derived by line-fitting three fairly broad Gaussian signals to the spectrum [18]. The plot in Fig. 9 represents the amorphous content of cellulose isolated from *Populus* and switchgrass during DAP. The more solvent accessible amorphous regions are more prone to degradation during pretreatment. Therefore, the changes observed in Fig. 9 more than likely correspond to the change detected in the MWD by GPC. Using a combination of ^{13}C relaxation experiments and NMR of cellulose undergoing solvent exchange it was suggested there are ^{13}C resonances that account for accessible or inaccessible fibril surfaces [52]. According to the spectral least-squared model developed as a result of this work, the amorphous content is described as solely comprised of fibril surfaces. However, by comparison with complementary dipolar WISE spectra on onion cell wall material, other researchers were able to conclude that bound water must be present inside cellulose fibrils [53]. This along with the observed GPC data suggests that some fraction of the intensity from the fibril surface resonances also include non-crystalline regions within the fibril interior mixed with crystalline regions on a relatively short length scale. This point is important because the fibril model used helps shape the interpretation of both the GPC and NMR data.

As residence time increases the amorphous content of *Populus* and switchgrass decreases with time. The *Populus* data points at a CSF value of ~1.75 and 2.54 indicate a decrease in

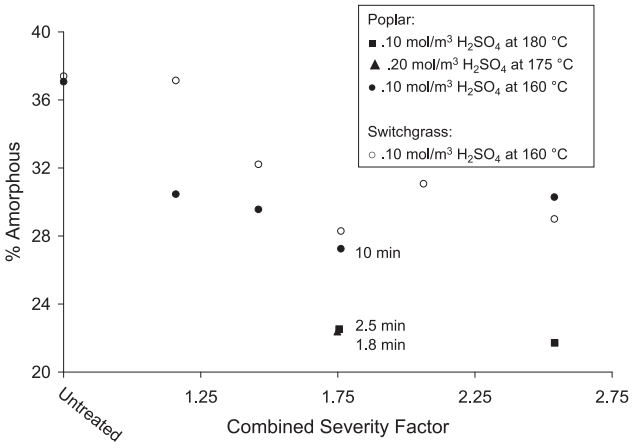

Fig. 9 – The amorphous content as determined by spectral fitting of the C_4 region of ^{13}C CPMAS spectra of isolated cellulose from poplar and switchgrass after pretreatment in dilute H_2SO_4 solution.

Please cite this article in press as: Foston M, Ragauskas AJ, Changes in lignocellulosic supramolecular and ultrastructure during dilute acid pretreatment of *Populus* and switchgrass, Biomass and Bioenergy (2010), doi:10.1016/j.biombioe.2010.07.023

Table 3 – Lateral fibril and fibril aggregate dimensions (nm) based on spectral fitting of the C_4 region in the ^{13}C CPMAS spectra of isolated cellulose from untreated and pretreated poplar and switchgrass.

Pretreatment time (min)	Pretreatment temp (°C)	H_2SO_4 (M)	CSF	Switchgrass		Poplar	
				LFD (nm)	LFAD (nm)	LFD (nm)	LFAD (nm)
Untreated	–	–	–	5.3	11.5	5.3	15.6
2.5	160	0.10	1.16	5.3	8.2	6.6	16.1
5	160	0.10	1.46	6.2	16.8	6.8	18.4
10	160	0.10	1.75	7.2	21.2	7.5	21.3
20	160	0.10	2.06	6.5	16.8	–	–
60	160	0.10	2.54	7.0	15.3	6.7	18.5
2.5	180	0.10	1.75	–	–	9.2	38.2
1.8	175	0.20	2.54	–	–	9.2	32.0
11	175	0.20	1.75	–	–	9.5	33.5

amorphous content may occur with temperature increase. This experimental observation can easily be explained, considering hydrolysis of cellulose is thermally accelerated. With a variety microscopy technique that confirm the existent of fibrils and fibril aggregates in cellulose and NMR data, Wickholm interprets inaccessible fibril surfaces as fibril-to-fibril contacts [27,52]. They showed utilizing this interpretation and a simple fibril model in which the fibril cross-section is square and the cross-sectional area of a cellulose chain is 0.55 nm^2/chain, that lateral fibril dimensions and lateral fibril aggregate dimensions could be determined.

3.3.3. *Cellulose fibril dimensions*

The average lateral fibril aggregate dimension (LFAD) and lateral fibril dimension (LFD) were estimated for the untreated and pretreated samples and the results are shown in Table 3. For both *Populus* and switchgrass, which displayed very similar trends with respect to LFAD and LFD, as the pretreatment time increases there is a corresponding decrease in the fibril surfaces and increase in interior order and fibril dimensions. The large amount of inaccessible fibril surface area typically seen in cellulose has been attributed to fibril distortions or dislocation [54]. Therefore, the existence of common crystallographic defects, such as edge or screw dislocations, increases the relative surface area to volume ratio of a cellulose fibril. This effect was observed during ball-milling of dry cellulose [55]. This work based on NMR data suggested ball-milling physically introduced crystal defects to cellulose fibrils, which increase the fibril surface area and the proportion of unordered cellulose. Upon re-wetting the cellulose interior order returned. It has been suggested water disrupts the strong hydrogen-bonding between fibril contacts allowing fibril dislocations to relax and decreasing the surface area to volume ratio [29,30,32,54,55].

Similarity, during DAP the removal and disruption of hemicellulose and lignin from the ultrastructure allows: (1) partial relaxation of fibril distortions, (2) additional degrees of freedom in the cellulose chain organization and (3) increased solvent induced swelling. This would reduce the relative surface area to volume ratio of a cellulose fibril and subsequently manifest as an increase in LFD. Work on the cross-sectional structure of the secondary wall of wood fibers suggests that under hydrothermal conditions a cellulose fibril and fibril aggregate is susceptible to enlargement due to thermally induced crystallization and aggregate growth. Thermally induced growth most likely is driven by the unfavorably high length-to-width ratio of the cellulose fibrils [48]. Under the proper conditions the fibrils within aggregates rearrange, on average thickening the aggregate to establish a more stable supramolecular conformation. Aggregate growth could account for the fairly constant LFAD/LFD ratio that persist with increasing residence time, which one may expect to decrease with residence time as hemicellulose is removed from within the fibril aggregate structure during DAP. Also the *Populus* samples at a CSF value of ~1.75 and 2.54 show an LFAD/LFD ratio that increases significantly with temperature, supporting the claims of thermally induced aggregate growth.

4. Conclusions

For the two biomass species examined, the hemicellulose components were hydrolyzed and solublized within ~5 min of pretreatment, beyond that cellulose begins to degrade. Based upon Klason lignin analysis, as DAP residence time is increased the amount of lignin solublization is minimal. Monitoring the MWD of pretreated cellulose suggests that most of the unwanted cellulose degradation occurs in the rapid initial phase of hydrolytic attack. In conjunction with NMR this initial phase of cellulose hydrolysis is localized to amorphous domains while the secondary phase occurs mainly at crystalline surfaces. There is also evidence that suggest a slow crystallization of amorphous cellulose happens, producing increased amounts of crystalline allomorphs at long pretreatment residence times and larger fibril dimensions. As temperature is increased the conversion from amorphous cellulose to crystalline structures decreases and the formation of less-ordered *para*-crystalline cellulose is increased. However, the more significant process occurring is related to the transformation of cellulose I_α to cellulose I_β and *para*-crystalline cellulose. We were also able to show DAP causes enlargement of cellulose fibrils and fibril aggregates. This was not only attributed to a thermally induced process thicken but also swelling and partial relaxation of fibril distortions. These results clearly demonstrate the complexity of processes occurring during pretreatment and seem to

Please cite this article in press as: Foston M, Ragauskas AJ, Changes in lignocellulosic supramolecular and ultrastructure during dilute acid pretreatment of *Populus* and switchgrass, Biomass and Bioenergy (2010), doi:10.1016/j.biombioe.2010.07.023

support the chemical and structural transformations predicted in Fig. 1.

Acknowledgments

This work was in part supported and performed as part of the BioEnergy Science Center. The BioEnergy Science Center is a U.S. Department of Energy Bioenergy Research Center supported by the Office of Biological and Environmental Research in the DOE Office of Science. This research was also funded by the Genomic Science Program, Office of Biological and Environmental Research in the DOE, under FWP ERKP752, a program headed by Barbara Evans at Oak Ridge National Lab to visualize lignocellulose through neutron scattering. In addition, we wish to thank the reviewers for their insightful comments.

REFERENCES

[1] Atalla RH. Cellulose "Comprehensive natural products chemistry". Amsterdam, Netherlands: Elsevier; 1999.
[2] Fengel D, Wegener G. Wood: chemistry, ultrastructure, reaction. New York: Walter de Gruyter; 1984.
[3] Nishiyama Y, Chanzy H, Langan P. Crystal structure and hydrogen-bonding system in cellulose Iβ from synchrotron X-ray and neutron fiber diffraction. J Am Chem Soc 2002;124:9074–82.
[4] Nishiyama Y, Sugiyama J, Chanzy H, Langan P. Crystal structure and hydrogen bonding system in cellulose Iα from synchrotron X-ray and neutron fiber diffraction. J Am Chem Soc 2003;125:14300–6.
[5] Chang M, Chou T, Tsao G. Structure, pretreatment and hydrolysis of cellulose "Bioenergy". Berlin: Springer; 1980.
[6] Pu Y, Zhang D, Singh P, Ragauskas A. The new forestry biofuels sector. Biofuels Bioprod Bioref 2008;2:58–73.
[7] Schell DJ, Farmer J, Newman M, McMillan JD. Dilute-sulfuric acid pretreatment of corn stover in pilot-scale reactor. Appl Biochem Biotechnol 2003;105–108:69–85.
[8] Soderstrom J, Galbe M, Zacchi G. Separate versus simultaneous saccharification and fermentation of two-step steam pretreated softwood for ethanol production. J Wood Chem Tech 2005;25:187–202.
[9] Soderstrom J, Pilcher L, Galbe M, Zacchi G. Two-step steam pretreatment of softwood by dilute H_2SO_4 impregnation for ethanol production. Biomass Bioenergy 2003;24:475–86.
[10] Mosier N, Wyman C, Dale B, Elander R, Lee Y, Holtzapple M, et al. Features of promising technologies for pretreatment of lignocellulosic biomass. Bioresour Technol 2005;96:673–86.
[11] Lee S, Kim I. Structural properties of cellulose and cellulase reaction mechanism. Biotechnol Bioeng 1983;XXV:3–51.
[12] Hsu T. Alcohol from cellulose. Chem Technol 1980;10:315–9.
[13] Pu Y, Ziemer C, Ragauskas A. CP/MAS ^{13}C NMR analysis of cellulase treated bleached softwood kraft pulp. Carbohydr Res 2006;341:591–7.
[14] VanderHart D, Atalla R. ^{13}C NMR spectra of cellulose polymorphs. J Am Chem Soc 1980;109:3249–50.
[15] VanderHart D, Atalla R. Observations by high-resolution carbon-13 nuclear magnetic resonance of cellulose I related to morphology and crystal structure. Macromolecules 1981;14:570–4.
[16] VanderHart D, Atalla R. Studies of microstructure in native celluloses using solid-state carbon-13 NMR. Macromolecules 1984;17:1465–72.
[17] VanderHart D, Atalla R. A composite of two distinct crystalline forms. Science 1984;223:283–5.
[18] Newman R, Hemmingston J. Carbon-13 NMR distinction between categories of molecular order and disorder in cellulose. Cellulose 1994;2:95–110.
[19] Lennholm H, Larsson T, Iversen T. Determination of cellulose I_α and I_β in lignocellulosic materials. Carbohydr Res 1994;261:119–31.
[20] Maunu S, Littia T, Kauliomaki S, Hortling B, Sundquist J. ^{13}C CPMAS NMR investigations of cellulose polymorphs in different pulps. Cellulose 2000;7:147–59.
[21] Larsson T, Westermark U, Iversen T. Determination of the cellulose I_α allomorph content in a tunicate cellulose by CP/MAS ^{13}C NMR spectroscopy. Carbohydr Res 1995;278.
[22] Larsson T, Wickholm K, Iversen T. A CP/MAS ^{13}C NMR investigation of molecular ordering in celluloses. Carbohydr Res 1997;302:19–25.
[23] Larsson T, Hult E, Wickholm K, Pettersson E, Iversen T. CP/MAS ^{13}C NMR spectroscopy applied to structure and interaction studies on cellulose I. Solid State Nucl Magn Reson 1999;15:31–40.
[24] Liitiä T. Application of modern NMR Spectroscopic techniques to structural studies of wood and pulp components. Helsinki, Finland: University of Helsinki, Department of Chemistry; 2002. p. 8–38.
[25] Ha M, Apperley D, Evans B. Fine structure in cellulose microfibrils: NMR evidence from onion and quince. Plant J 1998;16:183–90.
[26] Newman R. Estimation of the lateral dimensions of cellulose crystallites using ^{13}C NMR signal strengths. Solid State Nucl Magn Reson 1999;15:21–9.
[27] Wickholm K, Hult E, Larsson T, Iversen T, Lennholm H. Quantification of cellulose forms in complex cellulose materials: a chemometric model. Cellulose 2001;8:139–48.
[28] Huex L, Dinand E, Vignon MR. Structural aspects in ultrathin cellulose microfibrils followed by ^{13}C CPMAS NMR. Carbohydr Polym 1999;40:115–24.
[29] Virtanen T, Maunu SL, Tamminen T, Hortling B, Liitia T. Changes in fiber ultrastructure during various kraft pulping conditions evaluated by ^{13}C CPMAS NMR spectroscopy. Carbohydr Polym 2008;73:156–63.
[30] Hult E, Larsson T, Iverson T. A comparative CP/MAS ^{13}C NMR study of cellulose structure in spruce wood and kraft pulp. Cellulose 2000;7:35–55.
[31] Hult E, Larsson T, Iverson T. Cellulose fibril aggregation – an inherent property of kraft pulps. Polymer 2001;42:3309–14.
[32] Hult E, Larsson T, Iverson T. A Comparative CP/MAS ^{13}C NMR study of the supermolecular structure of polysaccharides in sulphite and kraft pulps. Holzforschung 2002;56:179–84.
[33] Hult E, Liitia T, Maunu S, Hortling B, Iverson T. A CP/MAS 13C-NMR study of cellulose structure on the surface of refined kraft pulp fibers. Carbohydr Polym 2002;49:231–4.
[34] Hult E, Iverson T, Sugiyama J. Characterization of the supermolecular structure of cellulose in wood pulp fibres. Cellulose 2003;10:103–10.
[35] Davis M. A rapid modified method for compositional carbohydrate analysis of lignocellulosics by high pH anion exchange chromatography with pulsed amperometric detection (HPAEC/PAD). J Wood Chem Technol 1998;18:235–52.
[36] Schroeder L, Haigh F. Gel permeation chromatographic analysis of cellulose and wood pulp polysaccharides. Appleton, Wisconsin: Institute of Paper Chemistry; 1979 March.
[37] Negro M, Manzanares P, Oliva J, Ballesteros I, Ballerteros M. Changes in various physical/chemical parameter of *Pinus*

Please cite this article in press as: Foston M, Ragauskas AJ, Changes in lignocellulosic supramolecular and ultrastructure during dilute acid pretreatment of *Populus* and switchgrass, Biomass and Bioenergy (2010), doi:10.1016/j.biombioe.2010.07.023

pinaster wood after stream explosion pretreatment. Biomass Bioenergy 2003;25:301–8.
[38] Li J, Henriksson G, Gellerstedt G. Lignin depolymerization/repolymerization and its critical role for delignification of aspen wood by steam explosion. Bioresour Technol 2007;98:3061–8.
[39] Lloyd T, Wyman C. Combined sugar yields for dilute sulfuric acid pretreatment of corn stover followed by enzymatic hydrolysis of the remaining solids. Bioresour Technol 2005;96:1967–77.
[40] Barth H, Regnier F. High-performance gel permeation chromatography of water-soluble cellulosics. J Chromatogr 1980;192:275–93.
[41] Segal L. Characterization of cellulose by gel permeation chromatography. J Polym Sci C 1968;21:267–82.
[42] Stephens C, Whitmore P, Morris H, Bier M. Hydrolysis of the amorphous cellulose in cotton-based paper. Biomacromolecules 2008;9:1093–9.
[43] Xiao B, Sun XF, Sun RC. Chemical, structural, and thermal characterizations of alkali-soluble lignins and hemicelluloses, and cellulose from maize stems, rye straw, and rice straw. Polym Degrad Stab 2001;74:307–19.
[44] Rinaudo M, Merle JP. Polydispersity of celluloses and enzymatic degraded celluloses by gel permeation chromatography. Euro Polym 1970;6:41–50.
[45] Emelsy A, Heywood R. On the kinetics of degradation of cellulose. Cellulose 1997;4:1–5.
[46] O'Sullivan A. Cellulose: the structure slowly unravels. Cellulose 1997;4:173–207.
[47] Hattula T. Effects of heat and water on the ultrastructure of wood cellulose. Helsinki, Finland: University of Helsinki, Department of Chemistry; 1985.
[48] Fahlen J, Salmen L. Cross-sectional structure of the secondary wall of wood fibers as affected by processing. J Wood Mater Sci 2003;38:119–26.
[49] Salem L. Thermal Softening of the components of paper: its effect on mechanical properties. Can Pulp Pap Assoc 1979;5:45–50.
[50] Back E, Salem L. Glass transitions of wood components hold implications for molding and pulping processes. Tappi J 1982;65:107.
[51] Irvine G. The glass transitions of lignin and hemicellulose and their measurement by differential thermal analysis. Tappi J 1984;5:118–21.
[52] Wickholm K, Larsson T, Iversen T. Assignment of non-crystalline forms in cellulose I by CP/MAS ^{13}C NMR spectroscopy. Carbohydr Res 1998;312:123–9.
[53] Hediger S, Lesage A, Emsley L. A New NMR method for the study of local mobility in solids and application to hydration of biopolymers in plant cell walls. Macromolecules 2002;35:5078–84.
[54] Josefsson T, Lennholm H, Gellerstedt G. Changes in cellulose supramolecular structure and molecular weight distribution during steam explosion of aspen wood. Cellulose 2002;00:1–8.
[55] Wormald P, Wickholm K, Larsson T, Iverson T. Conversions between ordered and disordered cellulose. Effect of mechanical treatment followed by cyclic wetting and drying. Cellulose 1996;3:141–52.

Please cite this article in press as: Foston M, Ragauskas AJ, Changes in lignocellulosic supramolecular and ultrastructure during dilute acid pretreatment of *Populus* and switchgrass, Biomass and Bioenergy (2010), doi:10.1016/j.biombioe.2010.07.023